Optical properties of singly charged conjugated oligomers: A coupled-cluster equation of motion study

A. Ye, Z. Shuai, O. Kwon, J. L. Brédas, and D. Beljonne

Citation: J. Chem. Phys. **121**, 5567 (2004); doi: 10.1063/1.1776113
View online: http://dx.doi.org/10.1063/1.1776113
View Table of Contents: http://jcp.aip.org/resource/1/JCPSA6/v121/i12
Published by the American Institute of Physics.

ARTICLES

Optical properties of singly charged conjugated oligomers: A coupled-cluster equation of motion study

A. Ye
Centre de Recherche en Electronique et Photonique Moléculaires, Service de Chimie des Matériaux Nouveaux, Université de Mons-Hainaut, Place du Parc 20, B-7000 Mons, Belgium and School of Chemistry and Biochemistry, Georgia Institute of Technology, Atlanta, Georgia 30332-0400

Z. Shuai
Laboratory of Organic Solids, Institute of Chemistry, The Chinese Academy of Sciences, 100080 Beijing, People's Republic of China

O. Kwon
School of Chemistry and Biochemistry, Georgia Institute of Technology, Atlanta, Georgia 30332-0400

J. L. Brédas and D. Beljonne
Centre de Recherche en Electronique et Photonique Moléculaires, Service de Chimie des Matériaux Nouveaux, Université de Mons-Hainaut, Place du Parc 20, B-7000 Mons, Belgium and School of Chemistry and Biochemistry, Georgia Institute of Technology, Atlanta, Georgia 30332-0400

(Received 18 December 2003; accepted 3 June 2004)

We have implemented a coupled-cluster equation of motion approach combined with the intermediate neglect of differential overlap parametrization and applied it to study the excited states and optical absorptions in positively and negatively charged conjugated oligomers. The method is found to be both reliable and efficient. The theoretical results are in very good agreement with experiments and confirm that there appear two subgap absorption peaks upon polaron formation. Interestingly, the relative intensities of the polaron-induced subgap absorptions can be related to the extent of the lattice geometry relaxations. © *2004 American Institute of Physics.*
[DOI: 10.1063/1.1776113]

I. INTRODUCTION

Since the discovery of conductive polymers by Heeger, MacDiarmid, and Shirakawa,[1] conjugated polymers and oligomers have attracted major interest due to their remarkable electronic and optical properties,[2] including photoluminescence and electroluminescence.[3–5] These properties lead to the possibility of using conjugated materials in a wide range of applications, such as light-emitting diodes (LEDs),[3,6–11] photodiodes,[12,13] and organic transistors.[14–16] To guide synthesis toward materials with improved performance, it is important to achieve a detailed understanding of their geometric and electronic structures at the molecular scale. In that respect, the comparison of experimental data with the results of quantum-chemical calculations can prove useful.

The study of conjugated oligomers is especially appealing since they can be obtained with high purity and well-defined chemical structure and conjugation length. In addition, oligomers are amenable to high-level correlated quantum-chemical methods, which have been shown to be essential to understand the photophysics of conjugated systems. The oligomer approach is thus convenient to investigate the fundamental electronic properties and nature of the excited states in neutral and doped conjugated materials.[17] This approach is further justified by the fact that the polymer chains can often be described as an array of conjugated segments interrupted by conformational (or chemical) defects.

Upon addition of positive or negative charges to the conjugated chains, new electronic states are created. These charges can result from chemical or electrochemical doping. Alternatively, an electric field, as applied in a LED or a transistor, can lead to injection of holes (positive charges) and electrons (negative charges) from the electrodes into the polymer or oligomer film. Charge injection gives rise to the appearance of spatially localized geometric defects, as a result of the strong electron-phonon coupling that is characteristic of conjugated chains.[18] In terms of condensed-matter physics, such charges coupled to a local lattice distortion of the backbone are described as positive or negative polarons.

The formation of polarons induces major modifications in the electronic structure of the conjugated chains: two new localized one-electron levels, i.e., a lower polaron level (POL1) and an upper polaron level (POL2), appear within the original gap, as shown in Fig. 1. For a singly positively (negatively) charged state, the lower (upper) polaron level is singly occupied. According to the one-electron band-structure model developed by Fesser, Bishop, and Campbell,[19] two new subgap optical transitions are expected in an oligomer: highest occupied molecular orbital (HOMO)→POL1 [POL2→LUMO (LUMO—lowest unoccupied molecular orbital)] and POL1→POL2.[20] Here, we apply coupled-cluster approach to the description of the optical properties of a wide range of conjugated systems in their singly charged state. Our goal is twofold: (i) to address the

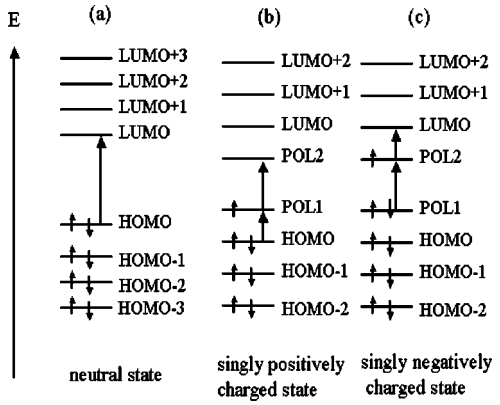

FIG. 1. Schematic single-particle representation of the absorption process in neutral (a), positively charged (b), and negatively charged (c) states.

accuracy of our approach for the calculation of polaron absorption spectra; indeed, a method that would be both tractable and reliable to calculate the excited states of charged systems is much in demand; and (ii) to explore the dependence on chemical structure of the polaron optical transition energies and intensities.

We report in this work a study of the optical properties of polarons in oligomers of polyacetylene (PA), polythiophene (PT), polyparaphenylene (PPP), and polyparaphenylene vinylene (PPV). The reason for this choice of materials is the following.

(i) Polyenes and polyacetylene are among the most studied conjugated systems and are usually considered as prototypical examples in model studies.

(ii) Studies of PT and its oligomers have opened the way to the design of optoelectronic devices with improved performance.[21] Oligothiophenes are currently incorporated in electronic or optoelectronic devices such as organic transistors,[14,15,22] light-emitting diodes,[23,24] and spatial light modulators.[25,26]

(iii) Phenylene-based materials, such as PPP or polyfluorenes, are widely used in light-emitting devices due to their high quantum efficiencies combined to improved stability,[27–32] they have been used in the fabrication of red-green-blue full color displays via color conversion techniques.[33]

(iv) PPV is the first and among the most efficient electroluminescent polymers. The fabrication of electroluminescent diodes based on PPV has been widely reported[3,6,34] and the nature of the lowest energy excited states in PPV has been the focus of many theoretical investigations.[35–37]

II. METHODOLOGY

One of the most used theoretical approaches to describe molecular excited states in quantum chemistry is configuration interaction (CI); configuration interaction singles (CIS) method has been widely exploited for the calculation of linear absorption spectra. In principle, the CI wave functions can be easily improved over the CIS approximation by including multiexcitation configurations, which allows for the inclusion of correlation effects to a larger extent but quickly faces the size-inconsistency issue. Full CI, though exact, is very much limited by the exponentially increasing dimensions of the Hilbert space. Although time dependent density functional theory (TD-DFT) might provide reasonable cation excitation energies,[38] it suffers from the shortcomings of ''pure'' (local density approximation) DFT methods that overshoot delocalization effects and fail to describe self-quenching of the charge induced by electron-phonon coupling.[39–42] The coupled-cluster (CC) method has been shown to provide accurate descriptions of electron correlation effects in many-body systems.[43–51] Bartlett and coworkers have widely extended the application scope of CCM to quantum chemistry.[52–59] The equation-of-motion coupled-cluster single and double excitations (EOM-CCSD) method is both size consistent and numerically efficient. We have shown previously that this approach provides an accurate description of the electronic structure and optical properties of conjugated materials in their neutral state.[60,61]

In this work, we apply the CCSD method to study the optical properties of a variety of charged conjugated oligomers. The ground-state geometry of these oligomers has been optimized with the semiempirical Hartree-Fock Austin Model 1 (AM1) method, which is known to provide good estimates of geometric structures for organic molecules.[62] The AM1 approach also yields a reasonable description of torsion potential energy curves when compared to those obtained by *ab initio* calculations.[63,64] The singly charged molecules are treated with the restricted open-shell Hartree-Fock approach, which better reproduces the localized nature of the geometry relaxations around the charge carriers than the unrestricted Hartree-Fock approach.[65] The transition energies and absorption cross sections of the singly positively and negatively charged species are simulated by combining the semiempirical intermediate neglect of differential overlap (INDO) parametrization[66,67] to the CCSD technique, on the basis of the AM1-optimized geometries (INDO/CIS results are also provided for comparison). Note that the INDO EOM-CCSD calculations are based on the INDO one-electron structure of the neutral systems. The Coulomb repulsion terms are expressed via the Mataga-Nishimoto potential.[68] For the neutral ground state, the close-shell restricted Hartree-Fock approach is applied. Below we give a brief overview of our implementation of the EOM-CCSD method for the calculation of closed-shell and open-shell systems.

A limited set of *ab initio* TD-DFT (the non-local Becke exchange and Lee-Yang-Parr correlation (BLYP) functional[69]) and CCSD calculations, both at the 6-31+G* basis set level, were also performed to assess the sensitivity of the excitation energies in the singly charged state of model systems on the used quantum-chemical approach.

A. Neutral state

The general electronic Hamiltonian for a molecule can be expressed as [in the following, indices $i,j,k,l,\ldots$ refer to occupied spin-orbitals (SOs); $a,b,c,d,\ldots$ to unoccupied molecular orbitals (MOs); and p, q, r, s to generic MOs]

$$H=\sum_{pq} h_{pq}p^{+}q+\frac{1}{4}\sum_{pqrs}\langle pq||rs\rangle p^{+}q^{+}sr. \tag{1}$$

The first term is the one-electron part, which includes the electron kinetic energy and the electron-nucleus interactions. The second term, the two-electron part, is given in the antisymmetric form: $\langle pq||rs\rangle=\langle pq|rs\rangle-\langle pq|sr\rangle$ and the two-electron integrals are defined as

$$\langle pq|rs\rangle=\int\int dr_1 dr_2 \varphi_p^*(r_1)\varphi_q^*(r_2)\frac{1}{r_{12}}\varphi_r(r_1)\varphi_s(r_2), \tag{2}$$

with φ denoting the MO wave function.

The CCSD ground state ansatz reads as

$$|\mathrm{CC}\rangle=\exp(T)|0\rangle, \tag{3}$$

where $|0\rangle$ is the Hartree-Fock ground-state determinant obtained from self-consistent field iterations; T consists in a linear combination of single and double excitations

$$T=T_1+T_2=\sum_{ia} t_i^a a^+ i+\sum_{i>j,a>b} t_{ij}^{ab} a^+ i b^+ j, \tag{4}$$

where the coefficients t are the amplitudes of the excitation configurations. The ground state is obtained by solving the following Schrödinger equation:

$$H\exp(T)|0\rangle=E_{\mathrm{CC}}\ \exp(T)|0\rangle. \tag{5}$$

Based on the CCSD ground state, we can construct the Heisenberg equation of motion within the configuration space by promoting one and two electrons from occupied to unoccupied MOs. The resulting equation is similar to a CI-like Schrödinger equation. We denote the excitation operators as μ, ν, σ, etc. The excited-state wave function is constructed as a linear combination of all single and double excitations on the CCSD ground state

$$|\mathrm{ex}\rangle=\sum_{\mu} R_\mu \exp(T)|\mu\rangle, \tag{6}$$

where $|\mu\rangle=\mu|0\rangle$ represents an excitation determinant and R_μ is the corresponding coefficient to be determined. The excited-state Schrödinger equation $H|\mathrm{ex}\rangle=E|\mathrm{ex}\rangle$ writes

$$H\sum_{\nu} R_\nu \exp(T)|\nu\rangle=E\sum_{\nu} R_\nu \exp(T)|\nu\rangle, \tag{7}$$

where E is the excited-state energy. When multiplying the above equation by $\exp(-T)$ from the left and then by an excitation bra configuration $\langle\mu|$, we obtain the following eigen-equation:

$$\sum_{\nu} \bar{H}_{\mu\nu}R_\nu=ER_\mu, \tag{8}$$

or

$$\sum_{\nu} (\bar{H}_{\mu\nu}-E_{\mathrm{CC}}\delta_{\mu\nu})R_\nu=(E-E_{\mathrm{CC}})R_\mu, \tag{9}$$

where E_{CC} is the CCSD ground-state energy, and

$$\begin{aligned}\bar{H}&=\exp(-T)H\exp(T)\\&=H+[H,T]+\tfrac{1}{2}[[H,T],T]+\tfrac{1}{6}[[[H,T],T],T]\\&\quad+\tfrac{1}{24}[[[[H,T],T],T],T]\end{aligned} \tag{10}$$

is the Hausdorff similarity transformed Hamiltonian. In principle, the expansion is infinite. However, in CCSD, the Hausdorff transformation terminates exactly after five terms because the Hamiltonian contains only one- and two-body terms.

It is convenient to extract the CCSD ground-state energy to give the following compact form:

$$AR=E_{\mathrm{ex}}R, \tag{11}$$

where $E_{\mathrm{ex}}=E-E_{\mathrm{cc}}$ and $A_{\mu\nu}=\bar{H}_{\mu\nu}-E_{\mathrm{CC}}\delta_{\mu\nu}$. The A matrix is a Jacobian matrix which can be diagonalized to give rise to the excited states.

Because the similarity transformed Hamiltonian, or the Jacobian, is no longer Hermitian, (actually, within a real basis, the Jacobian matrix is not symmetric), one can associate each eigenvalue with a right and a left eigenvector. The left eigenvector is given by

$$\langle\mathrm{ex}|=\sum_{\mu}\langle\mu|L_\mu \exp(-T). \tag{12}$$

L_μ can be determined in a way similar to R_μ.

In order to evaluate a physically observable quantity, such as the electric dipole transition moments for the optical process, we also need the left eigenvector of the CCSD ground state, i.e., the so-called Λ state in the CCSD gradient theory,[70] which is defined as

$$\langle L_0|=\langle 0|(1+\Lambda)\exp(-T), \tag{13}$$

where

$$\Lambda=\sum_{ia}\lambda_a^i i^+ a+\sum_{i>j,a>b}\lambda_{ab}^{ij} i^+ a j^+ b \tag{14}$$

is the deexcitation operator. The amplitude λ is determined by the Schrödinger equation of the Λ state

$$\begin{aligned}\langle L_0|H&=\langle 0|(1+\Lambda)\exp(-T)H\\&=\langle 0|(1+\Lambda)\exp(-T)E_{\mathrm{CC}}.\end{aligned} \tag{15}$$

B. Positively charged states

We apply the ionization potential (IP)-EOM-CCSD method[71] to investigate the positively charged states. When an electron is extracted from a molecule, one can form the following set of positively charged configurations:

$$|\sigma\rangle=\{k,c^+kl,c^+d^+klm\}, \tag{16}$$

where indices k, l, m refer to occupied MOs and c, d refer to unoccupied MOs. Then, the eigenstates can be expressed as:

$$|p\rangle=\sum_{\sigma} X_\sigma \exp(T)|\sigma\rangle, \tag{17a}$$

$$\langle p|=\sum_{\sigma}\langle\sigma|Y_\sigma \exp(-T). \tag{17b}$$

To derive the eigenvalue equation, we insert Eq. (17a) into the Schrödinger equation $H|p\rangle=E|p\rangle$ and extract the CC ground-state energy. We then obtain

$$(H-E_{cc})\sum_{\sigma} X_{\sigma} \exp(T)|\sigma\rangle$$

$$=(E-E_{cc})\sum_{\sigma} X_{\sigma} \exp(T)|\sigma\rangle. \quad (18)$$

When multiplying the above equation by $\exp(-T)$ from the left and then by $\langle\sigma|$, the following eigenvalue equation is derived:

$$\sum_{\rho} (\bar{H}_{\sigma\rho}-E_{CC}\delta_{\sigma\rho})X_{\rho}=\Delta E X_{\sigma}, \quad (19a)$$

where $\Delta E=E-E_{CC}$ is the IP. The eigenvalue equation for Y_{σ} is obtained in a similar way

$$\sum_{\sigma} Y_{\sigma}(\bar{H}_{\sigma\rho}-E_{CC}\delta_{\sigma\rho})=\Delta E Y_{\rho}. \quad (19b)$$

C. Negatively charged states

We apply electron attachment (EA)-EOM-CCSD[55] to investigate the negatively charged states. When adding an electron to a neutral closed shell, we can construct the configuration space as

$$|\nu\rangle=\{d^+, e^+d^+k, g^+c^+d^+kl\}. \quad (20)$$

Then, the eigenstates are expanded within this subspace as

$$|n\rangle=\sum_{\nu} U_{\nu} \exp(T)|\nu\rangle, \quad (21a)$$

$$\langle n|=\sum_{\nu} \langle\nu|V_{\nu} \exp(-T). \quad (21b)$$

For the negatively charged states, we write the eigenvalue equations for U_{ν} and V_{ν} as

$$\sum_{\mu} (\bar{H}_{\mu\nu}-E_{CC}\delta_{\mu\nu})U_{\mu}=\Delta E' U_{\nu}, \quad (22a)$$

$$\sum_{\mu} V_{\mu}(\bar{H}_{\mu\nu}-E_{CC}\delta_{\mu\nu})=\Delta E' Y_{\nu}, \quad (22b)$$

where $\Delta E'=E-E_{CC}$ is the electron affinity (EA).

Note that, for both the positive and negative polarons, a set of frontier π orbitals is included in the calculation of single (t_i^a) and double (t_{ij}^{ab}) excitation coefficients. For single excitations: all π orbitals are taken into account in polyenes; for n-ring oligophenylenes and oligothiophenes, the $2n$ highest occupied and $2n$ lowest unoccupied π orbitals are involved; for n-ring oligo(phenylenevinylene)s, the $3n-3$ frontier occupied π orbitals and $3n-3$ frontier unoccupied π orbitals are considered in the active space. For double excitations: the number of active molecular orbitals is divided by two for practical reasons related to computing demand.

D. Optical absorption spectra

The matrix element of the dipole operator between the lowest charged state (i.e., the ground state of the charged species) and the mth charged excited state is

$$\langle C_1|\hat{\mu}|C_m\rangle=\sum_{\sigma\rho} Y_{\rho}X_{\sigma}\langle\rho|\exp(-T)\mu \exp(T)|\sigma\rangle$$

$$=\sum_{\sigma\rho} Y_{\rho}X_{\sigma}\bar{\mu}_{\sigma\rho}. \quad (23)$$

The absorption spectrum is simulated by using the following expression:

$$I(\omega)\sim\frac{\omega}{3}\mathrm{Im}(\alpha_{xx}+\alpha_{yy}+\alpha_{zz}), \quad (24)$$

where α_{xx}, α_{yy}, and α_{zz} denote the diagonal elements of the polarizability tensor

$$\alpha_{xx}=\sum_{m\neq 1}\frac{\langle C_1|\hat{\mu}_x|C_m\rangle\langle C_m|\hat{\mu}_x|C_1\rangle}{\langle C_1|C_1\rangle\langle C_m|C_m\rangle}\left(\frac{1}{E_m-E_1-\hbar\omega-i\Gamma}+\frac{1}{E_m-E_1+\hbar\omega-i\Gamma}\right). \quad (25)$$

Γ is the damping factor (inversely proportional to the excited-state lifetime), which is set to 0.05 eV in the present study.

III. OPTICAL ABSORPTION SPECTRA OF CHARGED OLIGOMERS

We have applied the CCSD approach introduced above to describe the nature of the electronic excitations in the singly charged states of a variety of conjugated oligomers: polyenes, oligothiophenes, oligophenylenes, and oligo(phenylenevinylene)s. First of all, in order to gauge the accuracy of various theoretical approaches to reproduce excitation energies in singly charged conjugated molecules, a set of model systems (ethylene, bithiophene, and terthiophene) for which both experimental and high-level *ab initio* CCSD multiconfigurational second-order perturbation theory and (CASPT2) results are available, has been investigated. Table I collects the energies for the lowest optical excitations in the charged state of these molecules, as predicted at the semiempirical INDO/EOM-CCSD, INDO/CIS, and *ab initio* CCSD (6-31+G*), CASPT2, and TD-DFT (6-31+G*) level. Overall, all these formalisms yield a reasonable agreement to experiment. We note, however, that the INDO/EOM-CCSD approach is found to provide a significant improvement over INDO/CIS in comparison to the experimental or the state-of-the-art *ab initio* CCSD or CASPT2 results. Since the semiempirical INDO/EOM-CCSD method is much more tractable than its *ab initio* counterpart and amenable to large size systems with a good accuracy, we have therefore opted for this technique in the following.

A. Polyenes

Due to the strong electron-phonon coupling, injection or removal of an electron leads to significant modifications in the geometric structure of the polyene backbone. As illustration, the changes in C-C bond lengths upon single oxidation are shown for $C_{20}H_{22}$ in Fig. 2. The C-C bond lengths are significantly modified. The lattice distortions are mostly located around the center of the chain and extend over about 16 Å (when considering a cutoff of 0.01 Å for changes in

TABLE I. Transition energies (in eV) to the lowest excited states in the radical cations of ethylene, bithiophene, and terthiophene, as calculated at the semiempirical INDO/EOM-CCSD, INDO/CIS, and *ab initio* CCSD, CASPT2, and TD-DFT level.

ethylene$^{+\bullet}$				
	INDO/CCSD	INDO/CIS	CCSD 6-31+G*[a]	TD-DFT (BLYP) 6-31+G*[b]
$1\,^2A_u$	3.01	2.64	3.17	3.26

bithiophene$^{+\bullet}$					
	INDO/CCSD	INDO/CIS	TD-DFT(BLYP) 6-31+G*	CASPT2[c]	Experiment
$1\,^2A_u$	1.47	1.37	1.65	1.54	
$2\,^2A_u$	2.30	2.43	2.07	1.95	2.10[d], 2.14[e]
$3\,^2A_u$	2.79	3.42	2.65	2.78	2.92[d,f], 2.95[e]

terthiophene$^{+\bullet}$					
	INDO/CCSD	INDO/CIS	TD-DFT (BLYP) 6-31+G*	CASPT2[g]	Experiment[h]
$1\,^2A_u$	1.23	0.92	1.65	1.31	1.46
$2\,^2A_u$	1.9	1.87	2.65	1.94	2.25

[a]Calculations performed with Q-CHEM (Ref. 72).
[b]Calculations performed with GAUSSIAN 98 (Ref. 73).
[c]Reference 74.
[d]References 75 and 76.
[e]Reference 77.
[f]Reference 78.
[g]Reference 75.
[h]Reference 79.

bond length with respect to the neutral state). In the middle of the chain, the single bonds are shortened while the double bonds are elongated, leading to a vanishing degree of bond-length alternation (BLA), defined as the difference between the lengths of consecutive single and double bonds); BLA then increases when moving away from the center and reaches the ground-state value towards the chain ends, as shown in Fig. 2.

The INDO/EOM-CCSD calculations indicate the appearance of two subgap absorption features in the absorption spectra of singly charged polyenes, which result from the lattice relaxation phenomena and the formation of polarons defects, as shown in Fig. 3. Interestingly, the calculated spectra show a very large cross section for the higher-lying transition while the lower-lying optically allowed excitation carries a very weak intensity. This is fully consistent with the experimental results discussed by Bally *et al.* for the radical cations of *tert*-butyl-capped polyenes.[80] They conclude that such an intensity distribution arises from configuration mixing, a feature that is confirmed by the detailed CI analysis presented below.

The relative intensities of the two absorption bands can be understood from the following wave function analysis. The transition moment from the ground state, $|\text{state}_1\rangle$, to the excited state n, $|\text{state}_n\rangle$, of the singly charged molecule writes

$$\langle \text{state}_1|\hat{\mu}|\text{state}_n\rangle = \sum_{\sigma\nu} L_\sigma^1 R_\nu^n \langle \sigma|e^{-T}\hat{\mu}e^T|\nu\rangle = \sum_{\sigma\nu} L_\sigma^1 R_\nu^m \langle \sigma|\overline{\mu}|\nu\rangle = \sum_{\sigma\nu} L_\sigma^1 R_\nu^m \mu_{\sigma\nu}. \tag{26}$$

Because the ground-state wave function for the polaron is dominated by the configuration where an electron is removed from the HOMO (H) for the positively charged state ($L_1^1 \sim 0.95$), or an electron added to the LUMO (L) for the negatively charged state), Eq. (26) can be simplified as

$$\langle \text{state}_1|\hat{\mu}|\text{state}_n\rangle \sim \sum_\nu R_\nu^n \overline{\mu}_{1\nu}. \tag{27}$$

For the positively charged molecule, the two relevant excited states are dominated by the HOMO→POL1 (P1) and POL1→POL2 (P2) excitations. When only retaining expansion coefficients $R_{H,P1}$ and $R_{P1,P2}$, Eq. (27) can be simplified as

$$\langle \text{state}_1|\hat{\mu}|\text{state}_n\rangle \sim -R_{H\to P1}\mu_{H,P1} + R_{P1\to P2}\mu_{P1,P2}, \tag{28}$$

where $\mu_{i,j}$ is the dipole in MO basis. Note that $\langle \text{state}_1|\mu|\text{state}_n\rangle$ involves a destructive interaction between the two main configurations if the signs of $R_{H\to P1}\mu_{H,P1}$ and $R_{P1\to P2}\mu_{P1,P2}$ are the same and a constructive interaction if the signs are different.

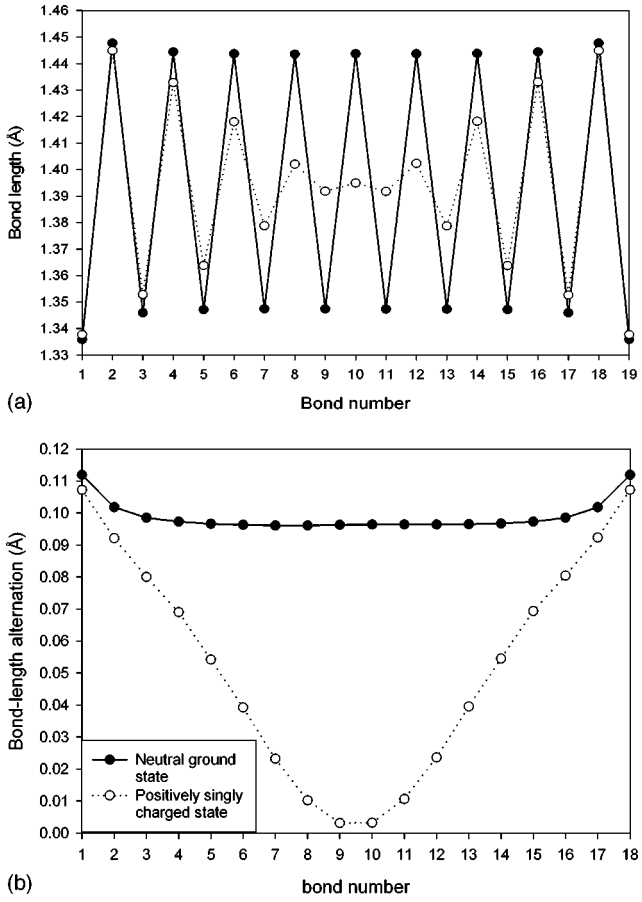

FIG. 2. AM1-optimized C-C bond lengths (top) and bond-length alternation (bottom) for $C_{20}H_{22}$ in the neutral (filled circles) and singe positively charged (open circles) states.

For negatively charged states, the two relevant excited states are dominated by the POL2→LUMO and POL1→POL2 excitations. When only retaining expansion coefficients $R_{P2,L}$ and $R_{P1,P2}$, Eq. (27) can be simplified as

$$\langle \text{state}_1|\hat{\mu}|\text{state}_n\rangle \sim R_{P2\rightarrow L}\mu_{P2,L}+R_{P1\rightarrow P2}\mu_{P1,P2}. \quad (29)$$

In contrast to the positively charged states, $\langle \text{state}_1|\mu|\text{state}_n\rangle$ involves a constructive interaction between the two main configurations if the signs of $R_{H\rightarrow P1}\mu_{H,P1}$ and $R_{P1\rightarrow P2}\mu_{P1,P2}$ are the same and a destructive interaction if the signs are different.

A detailed description of the main contributions for the excited states of singly charged polyenes is presented in Table II. For the first optical transition of the positively (negatively) charged polyenes, $R_{H\rightarrow P1}(R_{P2\rightarrow L})$ increases with increasing chain length while $R_{P1\rightarrow P2}$ decreases. Thus, in the long chain limit, the excited state leading to the first peak mainly originates from the electronic HOMO→POL1 (POL2→LUMO) transition. The oscillator strength associated with this excited state is small because the signs of $R_{H\rightarrow P1}\mu_{H,P1}(R_{P2\rightarrow L}\mu_{P2,L})$ and $R_{P1\rightarrow P2}\mu_{P1,P2}$ are the same (different), therefore leading to a partial cancellation of the transition dipoles. For the second transition, $R_{H\rightarrow P1}(R_{P2\rightarrow L})$ decreases with increasing chain length while $R_{P1\rightarrow P2}$ increases. For long polyene chains, the second absorption peak mainly arises from the electronic POL1→POL2 excitation.

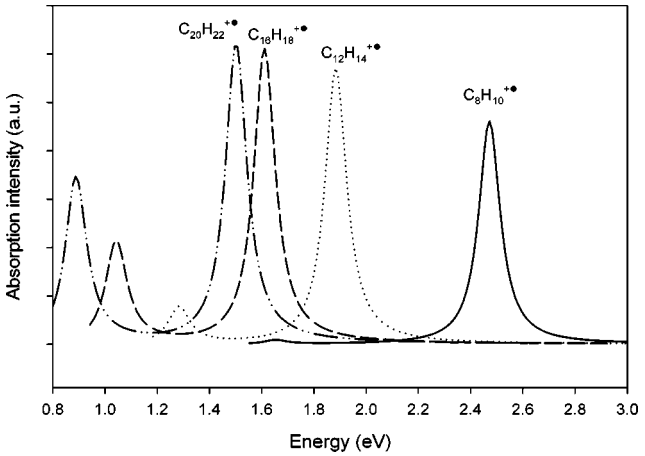

FIG. 3. INDO/EOM-CCSD absorption spectra of positively charged polyenes.

Because the signs of $R_{H\rightarrow P1}\mu_{H,P1}(R_{P2\rightarrow L}\mu_{P2,L})$ and $R_{P1\rightarrow P2}\mu_{P1,P2}$ are different (the same), the transition moments add up constructively and the resulting oscillator strength is large. Thus, as described by Bally *et al.*,[80] the relative intensities of the two polaronic peaks calculated for polyenes chains can be rationalized by the destructive (for the first band) and constructive (for the second band) combination of the HOMO→POL1 and POL1→POL2 configurations for the positive polaron (or the POL2→LUMO and POL1→POL2 configurations for the negative polaron).

In Fig. 4, we show the evolution of the lowest two optical transitions calculated by the INDO/EOM-CCSD method as a function of the inverse number of double bonds along the polyene chains. The theoretical results are found to agree very well with the experimental data reported by Bally and co-workers for the radical cations of *tert*-butyl-capped polyenes.[80] As expected from the increased π delocalization,

TABLE II. INDO/EOM-CCSD transition energies *E*, oscillator strengths O.S., and the major coefficients *R* of the lowest two energy absorption peaks for positive and negative polarons in polyenes.

			Major coefficients	
	Energy (eV)	O.S.	$R_{H\rightarrow P1}$	$R_{P1\rightarrow P2}$
$C_8H_{10}^{+\bullet}$	1.61	0.02	0.78	0.53
	2.59	1.15	0.66	−0.63
$C_{12}H_{14}^{+\bullet}$	1.26	0.19	0.89	0.32
	2	1.43	0.53	−0.70
$C_{16}H_{18}^{+\bullet}$	1.06	0.53	0.93	0.19
	1.66	1.52	0.34	−0.76
$C_{20}H_{22}^{+\bullet}$	0.93	0.86	0.94	0.12
	1.43	1.55	0.28	−0.77
			$R_{P2\rightarrow L}$	$R_{P1\rightarrow P2}$
$C_8H_{10}^{-\circ}$	1.27	0.07	0.87	−0.38
	2.45	0.98	0.50	0.75
$C_{12}H_{14}^{-\circ}$	1.08	0.22	0.91	−0.26
	1.83	1.28	0.42	0.75
$C_{16}H_{18}^{-\circ}$	0.97	0.44	0.93	−0.16
	1.61	1.35	0.33	0.75
$C_{20}H_{22}^{-\circ}$	0.83	0.67	0.93	−0.08
	1.42	1.40	0.25	0.76

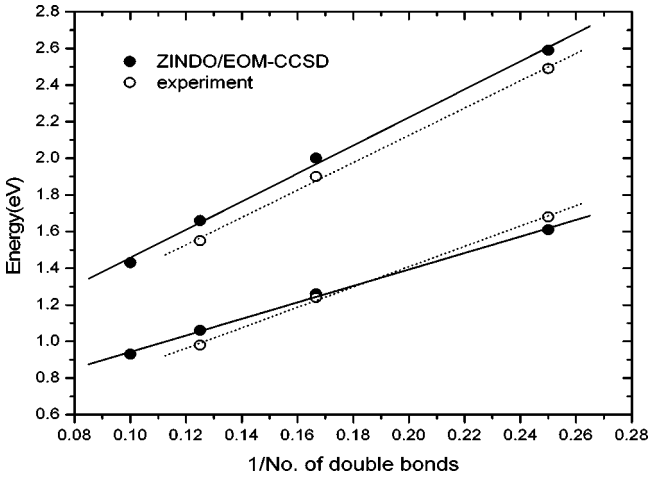

FIG. 4. Evolution of the lowest two energy transitions calculated by INDO EOM-CCSD, method, for positively charged polyenes as a function of the inverse number of double bonds. The filled triangles are the experimental results for the radical cations of *tert*-butyl-capped polyenes (taken from Ref. 80).

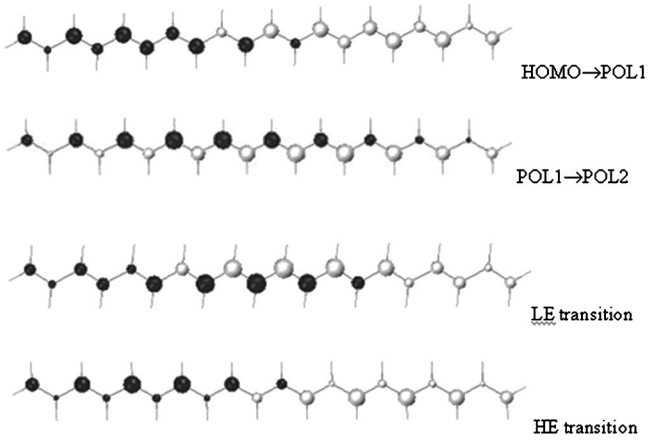

FIG. 5. EOM-CCSD transition densities for the pure excitations HOMO→POL1 and POL1→POL2 and for the excited states leading to the lower-energy (LE) transition and the higher-energy (HE) transition (from top to bottom) for the positive polaron in $C_{20}H_{22}$.

the peak positions are shifted to lower energies as the chain size increases and roughly follow a linear evolution with inverse number of repeating units.

In order to get further insight into the electron redistributions associated to the optical excitations, it is useful to have a look at the corresponding transition densities; these are defined as:[81]

$$\rho_{nn'}(r_1) = \int \psi_n^*(r_1, r_2, \ldots, r_M) \times \psi_{n'}(r_1, r_2, \ldots, r_M) dr_2 \cdots dr_M, \quad (30)$$

where M is the number of valence electrons included in the state wave functions; n and n' denote the initial and final states. Thus, the transition density diagrams represent the overlap between the initial and final wave functions of the states involved in the electronic transition. They can be regarded as providing a map of the reorganization in electronic density occurring upon excitation.

The transition densities for the pure excitations HOMO→POL1 and POL1→POL2 in the singly positively charged state of $C_{20}H_{22}$ are shown in Fig. 5 (black and light shadings correspond to increased and decreased charge density, respectively). We note that the POL1→POL2 transition corresponds to local redistributions (with successive positive and negative values), while the HOMO→POL1 excitation induces a significant charge separation over a large distance and therefore results in a larger transition moment (Table II). The transition densities for the excited states leading to the lower-energy (LE) and higher-energy (HE) transitions are also illustrated in Fig. 5. These are consistent with the analysis for the pure configurations; the important charge reorganization upon excitation to the upper-lying excited state leads to an intense absorption cross section for the HE peak while the weak intensity calculated for the LE peak stems from the more local shift in electronic density associated with excitation to the lower-lying state. It is interesting to note that, in the case of pure electronic configurations, the lowest optical transition (corresponding to HOMO→POL1 for a positive polaron and POL2→LUMO for a negative polaron) should be the most intense; however, when allowing these configurations to mix, it turns out that most of the oscillator strength is contained in the upper-lying excited state as a result of constructive interference, *vide supra*.

B. Oligothiophenes

The changes in geometric structure when going from the neutral to the charged form of oligothiophenes are similar to those calculated in polyenes.[82] Around the center of the molecules, the inter-ring C-C bond lengths get significantly shorter than those in the neutral geometry, while the thiophene rings adopt a quinoidic character. As a result, twisting of the rings around the inter-ring bonds is hindered. This leads to a planar configuration in the doped state.

The INDO/EOM-CCSD calculated absorption spectra of singly positively and negatively charged oligomers are illustrated in Fig. 6. These results are found to be in good agreement with the experimental data,[83] see Fig. 7. Both measurements and calculations indicate the emergence of two subgap

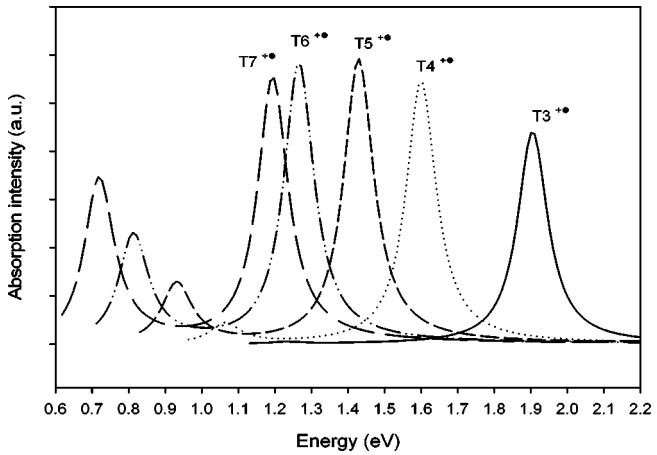

FIG. 6. INDO/EOM-CCSD absorption spectra for the positive polaron in oligothiophenes.

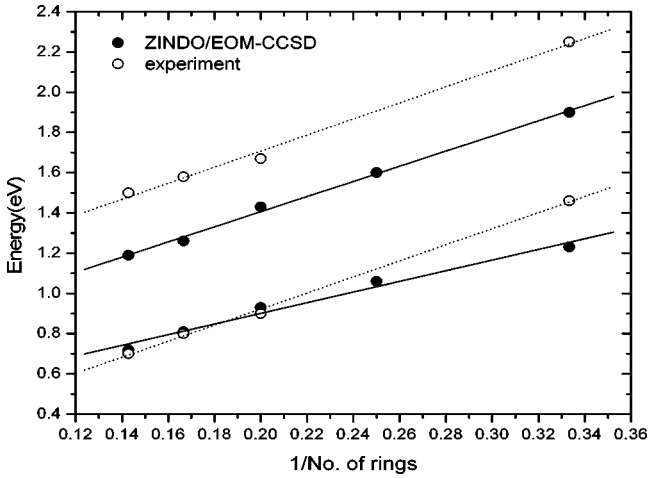

FIG. 7. Evolution of the lowest two energy transitions, as calculated by INDO/EOM-CCSD method, for the positive polarons in oligothiophenes as a function of the inverse number of thiophene rings (the experimental data are taken from Ref. 84).

absorption features, whose peak energies decrease almost linearly with the inverse number of repeat units. In addition, the first transition is found to be of lower intensity than the second one, especially in short oligomers. Similar conclusions were drawn from a combined experimental-theoretical investigation of the optical properties of charged 3,4-ethylenedioythiophene oligomers.[84]

From the analysis of the wave functions (Table III), it

TABLE III. INDO/EOM-CCSD transition energies, oscillator strengths O.S., and the major coefficients R of the lowest two energy absorption peaks for positive and negative polarons in oligothiophenes.

			Major coefficients	
Oligomer	Energy (eV)	O.S.	$R_{H\rightarrow P1}$	$R_{P1\rightarrow P2}$
$T2^{+\cdot}$	1.47	0.02	0.46	0.8
	2.3	0.32	0.76	−0.28
$T3^{+\cdot}$	1.23	0.01	0.73	0.59
	1.9	1.11	0.72	−0.58
$T4^{+\cdot}$	1.06	0.1	0.84	0.43
	1.6	1.37	0.61	−0.66
$T5^{+\cdot}$	0.93	0.32	0.9	0.29
	1.43	1.48	0.5	−0.72
$T6^{+\cdot}$	0.81	0.57	0.93	0.18
	1.26	1.45	0.41	−0.74
$T7^{+\cdot}$	0.72	0.86	0.94	0.1
	1.19	1.37	0.3	−0.77
			$R_{P2\rightarrow L}$	$R_{P1\rightarrow P2}$
$T2^{-\circ}$	1.28	0.04	0.82	−0.48
	2.32	0.58	0.53	0.76
$T3^{-\circ}$	1.06	0.09	0.85	−0.42
	1.89	0.92	0.36	0.54
$T4^{-\circ}$	0.91	0.19	0.89	−0.34
	1.63	1.16	0.46	0.76
$T5^{-\circ}$	0.81	0.34	0.92	−0.25
	1.5	1.34	0.4	0.77
$T6^{-\circ}$	0.71	0.52	0.93	−0.18
	1.33	1.39	0.33	0.78
$T7^{-\circ}$	0.65	0.65	0.94	−0.13
	1.27	1.36	0.26	0.78

TABLE IV. C-C bond lengths (in Å) in the neutral and positive polaron states of the five-ring oligophenylene, as optimized at the AM1 level. The AM1-calculated dihedral torsion angles for the positive polaron are indicated below each inter-ring bond.

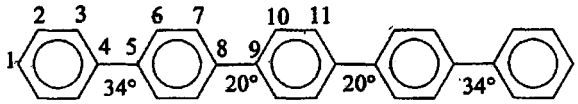

Bond	Neutral state	Positive polaron
1-2	1.395	1.395
2-3	1.393	1.393
3-4	1.403	1.405
4-5	1.461	1.454
5-6	1.402	1.411
6-7	1.391	1.382
7-8	1.402	1.420
8-9	1.461	1.428
9-10	1.391	1.426
10-11	1.402	1.373

can be concluded that the nature of the excited states leading to the lowest two optical transitions in oligothiophenes is very similar to the corresponding states in polyene. While the lower-lying excited state is mostly formed by a destructive interaction between the HOMO→POL1 and POL1→POL2 electronic configurations (for the positive polaron), the upper-lying state stems from a constructive interaction between the same excitations. However, the relative weights of these two configurations in the wave function expansion of the polaronic excited states differ more significantly in oligothiophenes than in polyenes. This effect is particularly pronounced in long thiophene oligomers, where the lowest-lying excited state is dominated by the HOMO→POL1 transition while the upper-lying state arises mostly from the POL1→POL2 excitation. As a consequence, with respect to the polyene case, there is a significant amount of oscillator strength transferred from the second to the first optical absorption feature in oligothiophenes.

C. Oligophenylenes and oligo(phenylene-vinylene)s

As for oligothiophenes, removing or adding an electron to oligophenylenes induces a significant relaxation in the conformation of the chains.[85] The amplitude of the inter-ring torsion angles are reduced with respect to the neutral state; however, because of strong steric hindrance between H atoms on adjacent rings, the torsion angles remain significantly different from zero in the polaronic geometries. For the sake of illustration, we show in Table IV the equilibrium bond lengths and torsion angles in the neutral and charged states of the five-ring phenylene (P5) oligomer. The optimized torsion angles around the central ring is calculated to be about 20° in the singly charged P5 oligomer, while the torsion angles involving the outer rings (~34°) are found to be closer to their neutral ground-state value (~40°).

The INDO/EOM-CCSD absorption spectra of singly positively charged phenylene oligomers are illustrated in Fig. 8. As for the other conjugated systems, the spectra show two dominant features. The evolution with inverse chain length

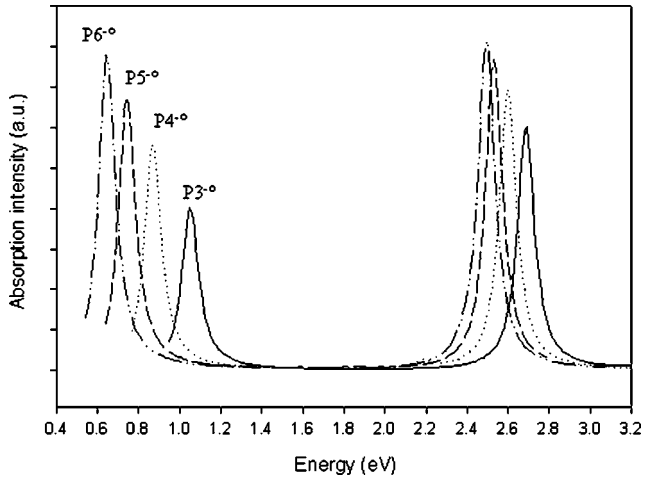

FIG. 8. INDO/EOM-CCSD absorption spectra of for the negative polaron in oligophenylenes.

of the two calculated optical excitations is compared to the corresponding evolution of the experimental data reported by Khanna *et al.*[86] in Fig. 9.

A detailed description of the main expansion coefficients obtained for the excited states of singly charged oligophenylenes is presented in Table V. In contrast to the situation encountered in polyenes and (to a lesser extent) oligothiophenes, the HOMO→POL1 (POL2→LUMO) configuration largely dominates the wave function expansion of the first transition in the positively (negatively) charged species. In addition, $R_{H\to P1}(R_{P2\to L})$ is only weakly affected by chain length. The oscillator strength for the second optically allowed excited state, which mainly originates in the electronic POL1→POL2 transition, is comparable to that of the first absorption band. In oligophenylenes, the transition moments from the ground state to the lowest two excited states are thus mainly dictated by the magnitude of the pure HOMO→POL1 (POL2→LUMO) and POL1→POL2 electronic configurations. This clearly shows up in the transition density diagrams, computed for the single excitations and the

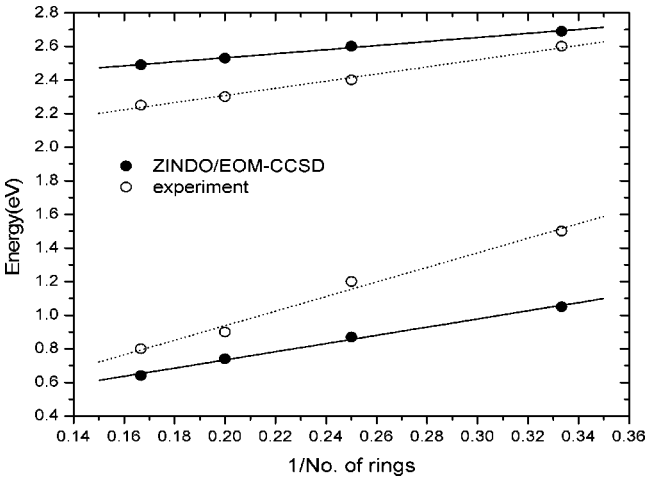

FIG. 9. Evolution of the lowest two energy transitions, as calculated by INDO/EOM-CCSD method, for the negative polarons in oligophenylenes, as a function of inverse number of phenylene rings (the experimental data are taken from Ref. 86).

TABLE V. INDO/EOM-CCSD transition energies, oscillator strengths O.S., and the major wave function coefficients *R* of the lowest two energy absorption peaks for positive and negative polarons in oligophenylenes.

			Major coefficients	
Oligomer	Energy (eV)	O.S.	$R_{H\to P1}$	$R_{P1\to P2}$
$P3^{+\bullet}$	1.38	0.5	0.96	0.17
	2.71	0.66	0.21	−0.8
$P4^{+\bullet}$	1.08	0.72	0.97	0.12
	2.61	0.71	0.15	−0.8
$P5^{+\bullet}$	0.88	0.88	0.97	0.11
	2.51	0.82	0.10	−0.82
$P6^{+\bullet}$	0.74	0.97	0.97	0.08
	2.46	0.77	0.07	−0.78
			$R_{P2\to L}$	$R_{P1\to P2}$
$P3^{-\circ}$	1.05	0.4	0.96	−0.15
	2.69	0.6	0.17	0.8
$P4^{-\circ}$	0.87	0.56	0.97	−0.11
	2.6	0.69	0.12	0.78
$P5^{-\circ}$	0.74	0.68	0.97	−0.09
	2.53	0.77	0.09	0.78
$P6^{-\circ}$	0.64	0.78	0.97	−0.07
	2.49	0.81	0.07	0.76

total excited-state wave functions (see Fig. 10). The weak mixing of these two configurations leads to two intense optical transitions. A very similar analysis holds for phenylenevinylene oligomers (Table VI). The INDO/EOM-CCSD absorption spectra of singly positively charged PPV oligomers are illustrated in Fig. 11. The theoretical results are compared to the experimental data of Schenk, Gregorius, and Müllen[87] in Fig. 12.

IV. DISCUSSION

The geometric deformations taking place upon charge injection in the inner part of representative oligomers ($C_{20}H_{22}$, T5, P5, and PPV5) are compared in Table VII; Δ is the change in bond length when going from the neutral state to the singly positively charge state. For polyenes and oligothiophenes, the amplitude of the bond-length modifications amounts to about 0.04 Å around the center of the charged defect; phenylene-based materials, oligophenylenes, and oligo(phenylenevinylene)s, give rise to lattice relaxations where the calculated changes in bond lengths are on the order of

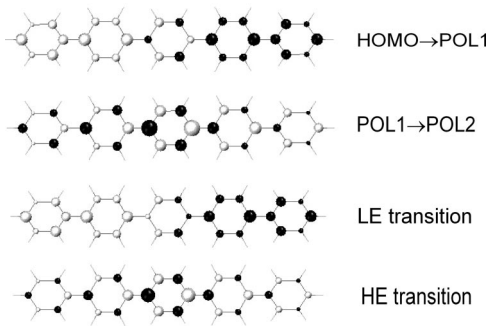

FIG. 10. Transition densities for the pure excitations HOMO→POL1 and POL1→POL2 and for the excited states leading to the LE and HE transitions (from top to bottom) for a positive polaron in the P5 oligomer.

TABLE VI. INDO/EOM-CCSD transition energies, oscillator strengths O.S., and the major wavefunction coefficients R of the lowest two energy absorption peaks for positive and negative polarons in oligo(phenylenevinylene)s.

			Major coefficients	
Oligomer	Energy (eV)	O.S.	$R_{H\rightarrow P1}$	$R_{P1\rightarrow P2}$
$PPV3^{+\bullet}$	1.07	0.67	0.95	0.17
	2.11	0.98	0.25	−0.77
$PPV4^{+\bullet}$	0.81	1.04	0.96	0.09
	1.97	1.02	0.15	−0.78
$PPV5^{+\bullet}$	0.63	1.29	0.96	0.06
	1.97	0.94	0.08	−0.72
$PPV6^{+\bullet}$	0.53	1.45	0.96	0.05
	1.92	1.04	0.07	−0.73
			$R_{P2\rightarrow L}$	$R_{P1\rightarrow P2}$
$PPV3^{-\circ}$	0.87	0.52	0.95	−0.16
	2.09	0.89	0.23	0.78
$PPV4^{-\circ}$	0.69	0.81	0.96	−0.09
	1.93	0.79	0.14	0.65
$PPV5^{-\circ}$	0.55	1	0.95	−0.07
	1.91	1.08	0.09	0.74
$PPV6^{-\circ}$	0.48	1.21	0.96	−0.05
	1.89	1.13	0.07	0.73

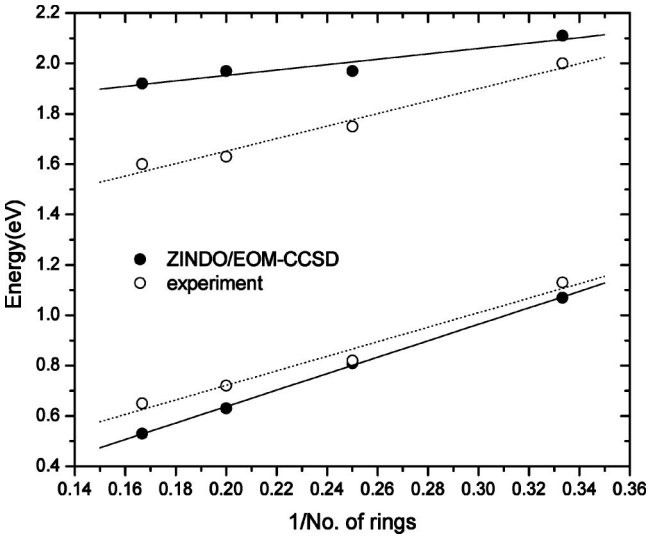

FIG. 12. Evolution of the lowest two energy transitions, as calculated by INDO/EOM-CCSD methods, for the positive polarons in oligo(phenylenevinylene)s, as a function of the inverse number of phenylene rings (the experimental data are taken from Ref. 87).

0.02 Å. The more rigid character of phenylene-based oligomers with respect to polyenes and oligothiophenes arises from the aromaticity of the phenylene rings.

In Table VIII, we present the AM1-optimized polaron size and chain length as well as their ratio γ (=polaron size/chain length), and the INDO/CCSD oscillator strengths computed for the two absorptions of $C_8H_{10}^{+\bullet}$, $C_{20}H_{22}^{+\bullet}$, $T3^{+\bullet}$, $T7^{+\bullet}$, $P3^{+\bullet}$, $P6^{+\bullet}$, $PPV3^{+\bullet}$ and $PPV6^{+\bullet}$. The γ value provides a measure of the degree of delocalization of the polaronic species. In $C_8H_{10}^{+\bullet}$ and $T3^{+\bullet}$, the polaron is found to delocalize nearly over the whole chain and the first peak is very weak. This leads to polaronic levels lying deep in the gap. As a consequence, the energies of the HOMO→POL1 (POL2→LUMO) and POL1→POL2 transitions are close and these configurations mix significantly leading to a weak LE transition (destructive combination of the two excitations) and a strong HE transition (constructive interaction). Note that γ decreases when the chain length increases as a result of the local character of the geometric deformation in the charged state; accordingly, an increase in the cross section for the LE peak is expected.

In contrast, phenylene-based materials lead to smaller distortions as illustrated by the smaller γ values. As a result, the polaronic levels are closer to the band edges; the HOMO→POL1 (POL2→LUMO) and POL1→POL2 transitions have very different energies; therefore, there is no significant wave function mixing. Both optical transitions then lead to two intense features in the optical absorption spectrum.

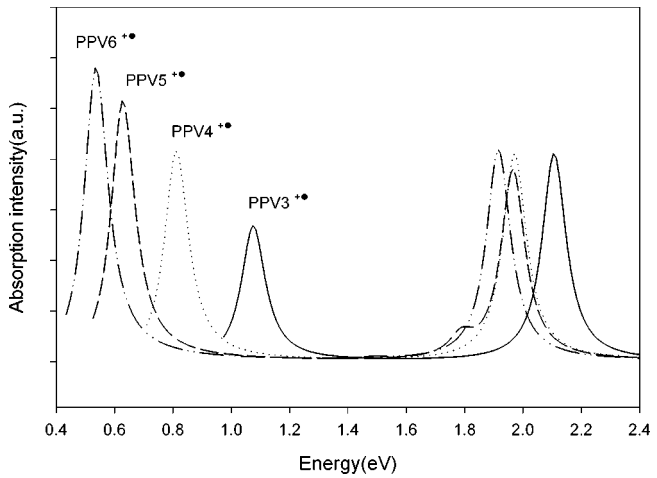

FIG. 11. INDO/EOM-CCSD absorption spectra for the positive polaron in oligo(phenylenevinylene)s.

TABLE VII. AM1-optimized geometry deformations in the central part of different oligomers: $C_{20}H_{22}$, T5, P5, and PPV5. The C-C bond lengths in the neutral state and the positive polaron state are given in Å; Δ is the change in bond length when going from the neutral state to the polaron.

Oligomer	Central part	Bond	Neutral state	Polaron	Δ
$C_{20}H_{22}$		1-2	1.444	1.395	−0.049
		2-3	1.347	1.392	0.045
T5	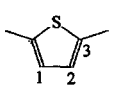	1-2	1.419	1.383	−0.036
		2-3	1.390	1.430	0.04
P5	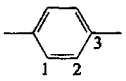	1-2	1.391	1.373	−0.018
		2-3	1.402	1.426	0.024
PPV5	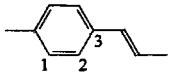	1-2	1.390	1.372	−0.018
		2-3	1.406	1.429	0.023

TABLE VIII. AM1-optimized polaron size, chain length, γ (=polaron size/chain length), and INDO/EOM-CCSD oscillator strengths for $C_8H_{10}^{+\bullet}$, $C_{20}H_{22}^{+\bullet}$, $T3^{+\bullet}$, $T7^{+\bullet}$, $P3^{+\bullet}$, $P6^{+\bullet}$, $PPV3^{+\bullet}$, and $PPV6^{+\bullet}$.

				Oscillator strength	
	Polaron size (Å)	Chain length (Å)	γ	LE peak	HE peak
$C_8H_{10}^{+\bullet}$	8.5	8.5	1	0.02	1.15
$C_{20}H_{22}^{+\bullet}$	16.0	25.6	0.63	0.86	1.55
$T3^{+\bullet}$	10.0	10.0	1	0.01	1.11
$T7^{+\bullet}$	17.2	25.4	0.68	0.86	1.37
$P3^{+\bullet}$	7.2	11.4	0.63	0.5	0.66
$P6^{+\bullet}$	11.5	24.2	0.47	0.97	0.77
$PPV3^{+\bullet}$	10.4	16.0	0.65	0.67	0.98
$PPV6^{+\bullet}$	17.0	35.8	0.47	1.45	1.04

V. SYNOPSIS

We have implemented a size-consistent correlated quantum-chemical approach, the EOM-CCSD method, to describe the charged excited states of conjugated materials. The transition energies and absorption intensities of the charged species were calculated by combining the semiempirical INDO method to the EOM-CCSD technique. In all cases, two subgap absorption features are found to dominate the optical spectrum, which are the characteristic optical signatures for polarons in conjugated materials. The relative intensities of these two bands and the dependence on chain length and chemical structure were analyzed. The theoretical results obtained on the basis of the AM1 polaronic geometries were found to agree very well with experimental data; this further confirms the picture that charged species in isolated conjugated chains self-localize due to strong electron-phonon coupling.[39,40,88] Furthermore, we found that the polaron is more localized in phenylene-based materials [oligophenylenes and oligo(phenylenevinylene)s] than in polyenes and oligothiophenes.

Interestingly, our calculations indicate that, in polyenes and oligothiophenes, most of the polaronic oscillator strength is concentrated in a single excited state while, in phenylene-based materials, the absorption cross-section is distributed nearly equivalently among two excited states. The description of these states is dominated by two electronic configurations: HOMO→POL1 (POL2→LUMO) and POL1→POL2 for a positively (negatively) singly charged state. These two configurations strongly interfere in polyenes and oligothiophenes, but only weakly in phenylene-based oligomers. As they provide contributions of opposite signs to the overall transition moment, the resulting oscillator strength is large for constructive interaction between the dipoles and weak for destructive interactions. This quantum interference phenomenon explains why one of the two polaronic absorptions has a small intensity in polyenes and oligothiophenes.

The mixing between these two configurations strongly depends on their relative energies as predicted from a simple two-state model (the closer in energy they are, the stronger their interaction). In that respect, the different behavior for the materials investigated in this work can be traced back to their relative ''rigidity'': large distortions take place in the doped polyenes and oligothiophene chains; this leads to the appearance of polaronic levels deep in the gap. Due to the aromaticity of the benzene rings, the geometric modifications are weakened in oligophenylenes and oligo(phenylenevinylene)s; the POL1 and POL2 levels are then closer to the band edges. As a result, the HOMO→POL1 (POL2→LUMO) and POL1→POL2 transitions have very different energies, which prevents significant wave function mixing and leads to two intense polaronic optical transitions.

ACKNOWLEDGMENTS

The work in Beijing was supported by NSFC Project No. 90203015 and the Ministry of Science and Technology ''973 program'' Project No. 2002CB613406. D.B. is a Senior Research Associate of the Belgian National Science Foundation (FNRS). The work in Mons was partly supported by the Belgian Federal Government Office for Scientific, Technological, and Cultural Affairs in the framework of the Inter-University Attraction Pole program P5/03, the European Commission ''STEPLED'' project, and FNRS. The work at the Georgia Institute of Technology was partly supported by the National Science Foundation (through the Science and Technology Program under Grant No. DMR-0120967 and through Grant No. CHE-0342321, DARPA, and the IBM Shared University Research Program. We thank Professor C. David Sherrill for the use of his Q-CHEM 2.0 software.

[1] H. Shirakawa, E. J. Louis, A. G. MacDiarmid, C. K. Chiang, and A. J. Heeger, Chem. Commun. (Cambridge) **16**, 578 (1977).
[2] *Handbook of Conducting Polymers, Second Edition, Revised and Expanded*, edited by T. A. Skotheim, R. L. Elsenbaumer, and J. R. Reynolds (Dekker, New York, 1998).
[3] J. H. Burroughes, D. D. C. Bradley, A. R. Brown, R. N. Marks, K. Mackay, R. H. Friend, P. L. Burn, and A. B. Holmes, Nature (London) **347**, 539 (1990).
[4] G. Gustafsson, Y. Gao, G. M. Treacy, F. Klavetter, N. Colaneri, and A. J. Heeger, Nature (London) **357**, 477 (1992).
[5] F. Hide, M. A. Diaz-Garcia, B. Schwartz, M. R. Andersson, Q. Pei, and A. J. Heeger, Science **273**, 1833 (1996).
[6] D. Braun and A. J. Heeger, Appl. Phys. Lett. **58**, 1982 (1991).
[7] Y. Ohmori, M. Uchida, K. Muro, and K. Yoshino, Jpn. J. Appl. Phys., Part 2 **30**, L1941 (1991).
[8] S. Tasch, A. Niko, G. Leising, and U. Scherf, Appl. Phys. Lett. **68**, 1090 (1996).
[9] R. H. Friend, R. W. Gymer, A. B. Holmes *et al.*, Nature (London) **397**, 121 (1999).
[10] Q. Pei, G. Yu, Ch. Zhang, Y. Yang, and A. J. Heeger, Science **269**, 1086 (1995).
[11] Q. Pei, Y. Yang, G. Yu, Ch. Zhang, and A. J. Heeger, J. Am. Chem. Soc. **118**, 3922 (1996).
[12] N. S. Sariciftci, L. Smilowitz, A. J. Heeger, and F. Wudl, Science **258**, 1474 (1992).
[13] J. J. M. Halls, C. A. Walsh, N. C. Greenham, E. A. Marseglia, R. H. Friend, S. C. Moratti, and A. B. Holmes, Nature (London) **376**, 498 (1995).
[14] F. Garnier, G. Horowitz, X. Peng, and D. Fichou, Adv. Mater. (Weinheim, Ger.) **2**, 592 (1990).
[15] F. Garnier, R. Hajlaoui, A. Yassar, and P. Srivastava, Science **265**, 1684 (1994).
[16] A. Dodabalapur, L. Torsi, and H. E. Katz, Science **268**, 270 (1995).
[17] *Electronic Material—The Oligomer Approach*, edited by G. Wegner and K. Müllen (VCH, Weinheim, 1998).
[18] J. L. Brédas and G. B. Street, Acc. Chem. Res. **18**, 309 (1985).
[19] K. Fesser, A. R. Bishop, and D. K. Campbell, Phys. Rev. B **27**, 4804 (1983).
[20] J. L. Brédas, Adv. Mater. (Weinheim, Ger.) **7**, 295 (1995).
[21] J. Roncali, Chem. Rev. (Washington, D.C.) **92**, 711 (1992).

[22] K. Waragai, K. Akimichi, S. Hotta, H. Kano, and H. Sasaki, Synth. Met. **57**, 4053 (1993).
[23] F. Geiger, M. Stoldt, H. Schweizer, P. Bauërle, and E. Umbach, Adv. Mater. (Weinheim, Ger.) **5**, 922 (1993).
[24] K. Uchiyama, H. Akimichi, S. Hotta, H. Noge, and H. Sasaki, Synth. Met. **58**, 63 (1994).
[25] D. Fichou, J. M. Nunzi, F. Charra, and N. Pfeffer, Adv. Mater. (Weinheim, Ger.) **6**, 64 (1994).
[26] D. D. C. Bradley, Phys. World **7**, 29 (1994).
[27] J. Stampfl, S. Tasch, G. Leising, and U. Scherf, Synth. Met. **71**, 2125 (1995).
[28] Y. Yang, Q. Pei, and A. J. Heeger, J. Appl. Phys. **79**, 934 (1996).
[29] G. Grem, G. Leditzky, B. Ullrich, and G. Leising, Adv. Mater. (Weinheim, Ger.) **4**, 36 (1992).
[30] W. Graupner, G. Grem, F. Meghdadi *et al.*, Mol. Cryst. Liq. Cryst. Sci. Technol., Sect. A **256**, 549 (1994).
[31] M. Era, T. Tsutsui, and S. Saito, Appl. Phys. Lett. **67**, 2436 (1996).
[32] G. Leising, S. Tasch, F. Meghdadi, L. Athouel, G. Froyer, and U. Scherf, Synth. Met. **81**, 185 (1996).
[33] S. Tasch, C. Brandstätter, F. Meghdadi, G. Leising, G. Froyer, and L. Athouel, Adv. Mater. (Weinheim, Ger.) **9**, 33 (1997).
[34] R. H. Friend, Synth. Met. **51**, 357 (1992).
[35] P. Gomes da Costa and E. M. Conwell, Phys. Rev. B **48**, 1993 (1993).
[36] Z. G. Soos, D. S. Galvao, and S. Etemad, Adv. Mater. (Weinheim, Ger.) **6**, 280 (1994).
[37] Z. Shuai, J. L. Brédas, and W. P. Su, Chem. Phys. Lett. **228**, 301 (1994).
[38] J. L. Weisman and M. Head-Gordon, J. Am. Chem. Soc. **123**, 11686 (2001).
[39] V. M. Geskin, A. Dkhissi, and J. L. Brédas, Int. J. Quantum Chem. **91**, 350 (2003).
[40] V. M. Geskin and J. L. Brédas, ChemPhysChem **4**, 498 (2003).
[41] L. Zuppiroli, A. Bieber, D. Michoud, G. Galli, F. Gygi, M. N. Bussac, and J. J. André, Chem. Phys. Lett. **374**, 7 (2003).
[42] S. Kuroda, K. Marumoto, H. Ito, N. C. Greenham, R. H. Friend, Y. Shimoi, and S. Abe, Chem. Phys. Lett. **325**, 183 (2000).
[43] H. J. Monkhorst, Int. J. Quantum Chem., Symp. **11**, 421 (1977).
[44] D. Mukherjee and P. K. Mukherjee, Chem. Phys. **39**, 325 (1979).
[45] J. Cizek and J. Paldus, Phys. Scr. **21**, 251 (1980).
[46] R. J. Bartlett, Annu. Rev. Phys. Chem. **32**, 359 (1981).
[47] K. Emrich, Nucl. Phys. A **351**, 379 (1981).
[48] C. D. Sherrill, A. I. Krylov, E. F. C. Byrd, and M. Head-Gordon, J. Chem. Phys. **109**, 4171 (1998).
[49] K. Raghavachari, G. W. Trucks, J. A. Pople, and M. Head-Gordon, Chem. Phys. Lett. **157**, 479 (1989).
[50] T. Van Voorhis and M. Head-Gordon, Chem. Phys. Lett. **330**, 585 (2000).
[51] A. I. Krylov, C. D. Sherill, and M. Head-Gordon, J. Chem. Phys. **113**, 6509 (2000).
[52] G. D. Purvis and R. J. Bartlett, J. Chem. Phys. **76**, 1910 (1982).
[53] H. Sekino and R. J. Bartlett, Int. J. Quantum Chem., Symp. **18**, 255 (1984).
[54] J. F. Stanton and R. J. Bartlett, J. Chem. Phys. **98**, 7029 (1993).
[55] M. Nooijen and R. J. Bartlett, J. Chem. Phys. **102**, 3629 (1995).
[56] S. R. Gwaltney, M. Nooijen, and R. J. Bartlett, Chem. Phys. Lett. **248**, 189 (1996).
[57] P. Piecuch, S. A. Kucharski, and R. J. Bartlett, J. Chem. Phys. **110**, 6103 (1999).
[58] J. Geertsen, M. Rittby, and R. J. Batlett, Chem. Phys. Lett. **164**, 57 (1989).
[59] S. Hirata, M. Nooijen, and R. J. Bartlett, Chem. Phys. Lett. **326**, 255 (2000).
[60] Z. Shuai and J. L. Brédas, Phys. Rev. B **62**, 15452 (2000).
[61] A. Ye, Z. Shuai, and J. L. Brédas, Phys. Rev. B **65**, 045208 (2002).
[62] M. J. S. Dewar, E. G. Zoebisch, E. F. Healy, and J. J. P. Stewart, J. Am. Chem. Soc. **107**, 3902 (1985).
[63] O. Lhost and J. L. Brédas, J. Chem. Phys. **96**, 5279 (1992).
[64] F. Demanze, J. Cornil, F. Garnier, G. Horowitz, P. Valat, A. Yassar, R. Lazzaroni, and J. L. Brédas, J. Phys. Chem. B **101**, 4553 (1997).
[65] J. Libert, J. L. Brédas, and A. J. Epstein, Phys. Rev. B **51**, 5711 (1995).
[66] J. A. Pople, D. L. Beveridge, and P. A. Dobosh, J. Chem. Phys. **47**, 2026 (1967).
[67] M. C. Zerner, G. H. Loew, R. F. Kichner, and U. T. Mueller-Wesrerhoff, J. Am. Chem. Soc. **102**, 589 (1980).
[68] N. Mataga and K. Nishimoto, Z. Phys. Chem. (Leipzig) **13**, 140 (1957).
[69] C.-P. Hsu, S. Hirata, and M. Head-Gordan, J. Phys. Chem. A **105**, 451 (2001).
[70] A. C. Scheiner, G. E. Scuseria, J. E. Rice, T. J. Lee, and H. F. Schaefer, J. Chem. Phys. **87**, 5361 (1987).
[71] J. F. Stanton and J. Gauss, J. Chem. Phys. **101**, 8938 (1994).
[72] J. Kong, C. A. White, A. I. Krylov *et al.*, Q-CHEM (version 2.0) Q-Chem, Inc., Export, PA (2000).
[73] M. J. Frisch, G. W. Trucks, H. B. Schlegel *et al.*, GAUSSIAN 98 (version A.11.3) Gaussian, Inc., Pittsburgh PA (2002).
[74] M. Rubio, E. Orti, R. Pou-Amerigo, and M. Merchan, J. Phys. Chem. A **105**, 9788 (2001).
[75] T. Keszthelyi, M. M.-L. Grage, J. F. Offersgaard, R. Wilbrandt, C. Svendsen, O. S. Mortensen, J. K. Pedersen, and H. J. A. Jensen, J. Phys. Chem. A **104**, 2808 (2000).
[76] T. Keszthelyi, M. M.-L. Grage, R. Wilbrandt, C. Svendsen, and O. S. Mortensen, Laser Chem. **19**, 393 (1999).
[77] C. H. Evans and J. Scaiano, J. Am. Chem. Soc. **112**, 2694 (1990).
[78] S. S. Emmi, M. D'Angelantonio, G. Beggiato, G. Poggi, A. Geri, D. Pietropaolo, and G. Zotti, Radiat. Phys. Chem. **54**, 263 (1999).
[79] V. Wintgens, P. Valat, and F. Garnier, J. Phys. Chem. **98**, 228 (1994).
[80] T. Bally, K. Roth, W. Tang, R. R. Schrock, K. Knoll, and L. Y. Park, J. Am. Chem. Soc. **114**, 2440 (1992).
[81] J. R. Heflin, K. Y. Wong, O. Zamani-Khamiri, and A. F. Garito, Phys. Rev. B **38**, 1573 (1988).
[82] J. Cornil, D. Beljonne, and J. L. Brédas, J. Chem. Phys. **103**, 842 (1995).
[83] J. Guay, P. Kasai, A. Diaz, R. Wu, J. M. Tour, and L. H. Dao, Chem. Mater. **4**, 107 (1992).
[84] J. J. Apperloo, L. Groenendaal, H. Verheyen *et al.*, Chem.-Eur. J. **8**, 2384 (2002).
[85] E. Zojer, J. Cornil, G. Leising, and J. L. Brédas, Phys. Rev. B **59**, 7957 (1999).
[86] R. K. Khanna, Y. M. Jiang, B. Srinivas, Ch.B. Smithhart, and D. L. Wertz, Chem. Mater. **5**, 1792 (1993).
[87] R. Schenk, H. Gregorius, and K. Müllen, Adv. Mater. (Weinheim, Ger.) **3**, 492 (1991).
[88] F. C. Grozema, L. P. Candeias, M. Swart, P. Th. van Duijnen, J. Wildeman, G. Hadziioanou, L. D. A. Siebbeles, and J. M. Warman, J. Chem. Phys. **117**, 11366 (2002).